

# Modelling of the compaction phase during Hot Isostatic Pressing process at the mesoscopic scale

A. ZOUAGHI<sup>a</sup>, M. BELLET<sup>a</sup>, Y. BIENVENU<sup>b</sup>, G. PERRIN<sup>c</sup>, D. CEDAT<sup>d</sup>, M. BERNACKI<sup>a</sup>

<sup>a</sup> MINES ParisTech, Centre for Material Forming (CEMEF), UMR CNRS 7635, BP 207, 06904 Sophia-Antipolis, France

<sup>b</sup> MINES ParisTech, Centre des Matériaux, UMR 7633, BP 87, 91003 Evry Cédex, France

<sup>c</sup> AREVA NP, Tour Areva, 92084 Paris La Défense, France

<sup>d</sup> AREVA NP, Technical center, BP 181, 71205 Le Creusot Cédex, France

---

## Abstract

During Hot isostatic pressing (HIP) of metal powder, power-law creep is the dominant mechanism during the densification process. However, the understanding of the global impact of the thermo-mechanical boundary conditions and of the powder granulometry on the microstructure obtained after this first mechanism is not straightforward. A finite element methodology based on the use of a level set framework coupled with a remeshing technique is proposed in order to model the viscoplastic deformation of powder particles during HIP at the mesoscopic scale thanks to a Representative Elementary Volume. The methodology consists in generating, in a finite element mesh, a sphere packing of particles by representing implicitly all particles by means of a limited set of level-set functions. Mesh adaptation is also performed at particle boundaries to describe properly the particles and to manage the discontinuity of the physical properties. Such 2D scale mesoscopic densification simulations are presented and discussed.

**Keywords:** HIP, powder densification, level-set function, remeshing technique, mesoscopic scale

---

## 1. Introduction

Because of opportunities that Hot Isostatic Pressing (HIP) offers in both technical and economic points of view, this process is increasingly used in industries for the manufacture of diverse engineering components. This technology allows the production of near-net-shape densified metal or ceramic parts. HIPing process consists of the application of an isostatic pressure through a gaseous or liquid medium to an out-gassed and canned powder mass at an elevated temperature. The modeling of HIP is an open and complex research problem as it is composed by several mechanisms that contribute simultaneously or successively to densification [Atkinson and Davis, 00]. To achieve a better understanding of the local heterogeneities, which can appear during HIP process, it is essential to develop computational models at both the macroscopic and the particles scales. During conventional HIPping, the first dominant mechanism taking place in the process is the plastic deformation of powder particles, which at such high temperature, can be reasonably addressed by power-law creep models. Then, when the temperature and pressure are ramped up in phase, several mechanisms like surfacic or volumic diffusion at the particles interfaces appear and become preponderant for the last percent of densification [Ransing and al., 00]. The influence of these mechanisms can be neglected in most of the time of compaction process. That's why, they will not be discussed in this article.

Today, thanks to considerable progress in computational and experimental domains, we can have access to microscopic information and model many processes at the mesoscopic and microscopic scale. Modeling at the REV scale can provide some clarification and explain about the prediction of the behavior of the manufactured parts by studying the impact of

process parameters (temperature, pressure, duration, granulometry, ...) on final characteristics. The overall main objectives of the work reported in this article are to model the preponderant mechanism at the beginning of HIP, which is the viscoplastic deformation of the particles, and to follow the kinetics of the densification at the REV scale. Powder compaction modeling on the particle scale has been treated by a numbers of research groups. These investigations are based on a finite element method or discrete element method or a combination between the two methods [Ransing and al., 00][ Gething and al., 06]. The finite element model is based on a force balance and ignores any effect of powder acceleration in a Lagrangean domain. Moreover, the inter-particle space is not meshed and a friction between powder and tool set is introduced [Ransing and al., 00]. In addition, the computational cost of these approaches is still a disadvantage especially in 3D. In this paper, a finite element strategy based on a level set framework, coupled with an adaptive automatic remeshing technique, to model the power compaction is presented. Moreover, a Eulerian framework is adopted and a multiphase flow problem is described in a single mesh domain which includes all sub-domains of the REV.

Hence, in this present paper, we shall first recall the governing equations of the mechanical problem, the constitutive laws adopted and boundary conditions applied. Then, the finite element model and the remeshing techniques are described. Afterwards, results are shown and discussed. Finally, we close with concluding remarks and possible future work.

## 2. Mechanical modeling

To simulate the consolidation of powder during HIP process at the mesoscopic scale, a REV, composed of 2D circular powder particles and inter-particle space (IPS), is considered. Modelling the particles deformation is one of the main goals of our work. Thus, in order to not follow the evolution of the IPS through boundaries of the domain, a Eulerian framework description is adopted.

### 2.1. Governing equations

The equations governing the mechanical behavior in the REV domain are the momentum and the mass conservation equations which can be written as:

$$\rho \frac{dv}{dt} = \nabla \cdot \sigma + \rho g \quad , \quad (1)$$

$$\frac{\partial \rho}{\partial t} + \nabla \cdot (\rho v) = 0 \quad , \quad (2)$$

where  $v$  is the velocity,  $\sigma$  the Cauchy stress tensor,  $\rho$  the density and  $g$  the gravity field.

### 2.2. Material behavior

A gas atomized 316L stainless steel powder has been selected for this study. It is generally assumed that the high temperature deformation mechanism of particles involves a power-law creep behavior [Choi and Gethin, 09], [Helle and al., 85], [Wilkinson and Ashby, 75] which can be described thanks to the classical following equation:

$$S = 2K(\sqrt{3}\dot{\epsilon})^{m-1} \dot{\epsilon} \quad , \quad (3)$$

where  $S$ ,  $\dot{\epsilon}$  and  $\dot{\epsilon}$  denote, respectively, the stress deviator tensor, the strain rate tensor and the equivalent strain rate.  $K$  is the metal consistency and  $m$  the strain rate sensitivity coefficient, both being temperature dependent. The temperature dependent material data for 316L powder are taken from references [Arzt and al., 83] and [Bouaziz and al., 97]. We take as hypothesis that the IPS behaves like a compressible Newtonian fluid ( $K = \eta$  and  $m = 1$  in equation (3)):

$$S = 2\eta dev(\dot{\epsilon}) \quad , \quad (4)$$

where  $\eta$  is the dynamic viscosity and  $dev(\dot{\epsilon})$  denotes the deviatoric part of  $\dot{\epsilon}$ .

### 2.3. Solution strategy

For a better consideration of the behavior of the IPS (vacuum in HIP), the method used is to introduce a compressibility term ( $C_K \dot{p}$ ) in the mass conservation equation. So the following equations are solved:

$$\rho \left( \frac{\partial v}{\partial t} + \nabla v \cdot v \right) = \nabla \cdot (2K(\sqrt{3}\dot{\epsilon})^{m-1} \dot{\epsilon}) - \nabla p + \rho g, \quad (5)$$

$$\nabla \cdot v + C_K \dot{p} = 0 \quad . \quad (6)$$

where  $\rho$ ,  $C_K$ ,  $K$  and  $m$  are introduced by a mixture law. To introduce the incompressibility of the powder particles, the value of the compressibility coefficient  $C_K = \epsilon'$  is considered very close to zero. Concerning the IPS, values of  $C_K$  are high ( $C_K \gg \epsilon'$ ) to take into account the compressibility of the medium.

Two types of boundary conditions (BC) are considered. As a first approach, an isotropic pressure is applied (Fig. 2). In a second approach, normal stress is applied on two encompassing domains and symmetry conditions are imposed on the two other boundaries of the REV (Fig. 1).

## 3. Numerical modeling

All numerical calculations mentioned in this paper were performed with the Cimlib finite element C++ library developed in Cemef.

### 3.1. Level set framework

In our approach, a level set method is used, in a finite element context, for describing the two media and the virtual tools used to impose the boundary conditions. The level set approach is a numerical method that enables to locate and to track surfaces or interfaces. Powder particles, the surrounding domain (SD) (which transmits all BCs to IPS and powder particles) and IPS are implicitly described using a signed distance function  $\alpha$ , to the interface of the considered object  $c$  [Coupez, 06]. Therefore, the interface  $\partial c$  is given implicitly by the zero isovalue of the level set function  $\alpha$ .

$$\alpha(x) = \begin{cases} d(x, \partial c) & \text{if } x \in c \\ 0 & \text{if } x \in \partial c \\ -d(x, \partial c) & \text{if } x \in \Omega - c. \end{cases} \quad , \quad (7)$$

For each node of the FE mesh, the level set function is evaluated. Then, it is possible to determine the function anywhere in the domain. In the first instance, taking into account that all particles have the same behavior and to avoid an important cost of computation, we worked with one level set function representing all powder particles. Assuming that each particle has a distance function  $\alpha_i(x)$  defining its interface, the function  $\alpha(x) = \max_i(\alpha_i(x))$  represents the global distance function that defines all powder particles. In fact, its zero value corresponds to the envelope of the union of all particles.

If a velocity  $v$  is applied, the motion of the interfaces (surfaces) is modeled thanks to the following convection-reinitialization equation:

$$\frac{\partial \alpha}{\partial t} + (v + \lambda U) \cdot \nabla \alpha = \lambda s B \quad , \quad (8)$$

$$\alpha(t=0, x) = \alpha_0(x) \quad ,$$

where  $\lambda$  is a parameter having the dimension of a velocity and depending on mesh size and time step,  $U$  a vector defined by  $U = s \frac{\nabla \alpha}{L_{\min} + (1 - L_{\min})|\nabla \alpha|}$ ,  $B = \sqrt{1 - \left(\frac{\pi \alpha}{2E}\right)^2}$  which represents a calculated parameter in the solver,  $L_{\min}$  and  $E$  two parameters defined as ( $h_{\text{mesh}} < L_{\min} < 2 \cdot h_{\text{mesh}}$ ) and ( $10 \cdot h_{\text{mesh}} < E < 20 \cdot h_{\text{mesh}}$ ) where  $h_{\text{mesh}}$  represents local mesh size at the interfaces in the orthogonal direction and  $s$  is the sign of  $\alpha$ .

### 3.2. Mixture law

It should be noted that, in this paper, a multiphase flow problem (gas and solid phases) is described. Parameters of the mechanical problem are so defined by a mixture law. To illustrate, let us consider two level-set functions: the first characterizing the interface of particles powder and the second the interface of the SD, the mixture law for a parameter  $M$  can be expressed as:

$$\langle M \rangle = [f_1(\alpha)M_{\text{particle}} + (1 - f_1(\alpha))M_{\text{IPS}}] (1 - f_2(\alpha)) + f_2(\alpha)M_{\text{SD}} \quad , \quad (9)$$

The choice of the two characteristics functions  $f_1(\alpha)$  and  $f_2(\alpha)$  is very important because it controls the transition of the physical subdomains characteristics.

### 3.3. Remeshing algorithm

The accuracy of the finite element method depends on the size of the elements. The smaller these elements, the more accurate will be the results. For evident reasons of computational cost, we cannot refine uniformly all the domain. But, it is possible to optimize the mesh by refining only in useful area and coarsening the mesh outside of this area. So a good adaptive remeshing strategy is needed to perform a good description and accuracy of particles interfaces. The computational cost of our model is reduced thanks to an appropriate mesh refinement around the interfaces. In this paper, a predetermined mesh generation is used. In this technique, the size of the mesh refinement which takes place in a narrow zone surrounding the solid-IPS interface is chosen by the user [Bernacki and al., 09]. Furthermore, in HIP, the material undergoes large deformation so remeshing is required in order to avoid a loss of accuracy. Thus, as the interfaces move due to particles deformation, periodic remeshing is performed such that the refinement zone always coincides with the interface position.

## 4. Numerical results

The first test case modeled corresponds to the compaction of 2D circular powder particles in a square REV taking into account an isothermal condition ( $m$  and  $K$  material parameters are considered constant) (Fig.1). This work has permitted to develop a numerical strategy to model the compaction of a set of 2D powder particles at a constant temperature subjected to velocity or isostatic pressure or stress boundary condition. Moreover, it is important to emphasize that the proposed framework was also applied to other microstructures involving a great numbers of monodisperse or polydisperse particles. An initial microstructure generator, introduced in CimLib, permits to generate complex 2D and 3D statistical virtual microstructures in a finite element (FE) context [Hitti and al., 12]. An optimization technique has been used to suppress unphysical voids encountered when using an advancing front method [Bernacki and al., 09].

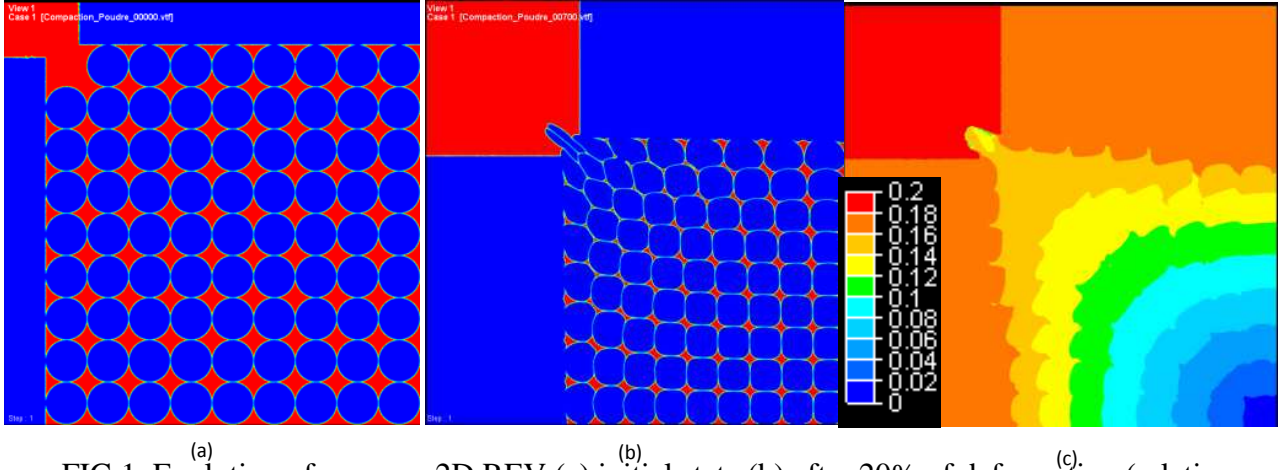


FIG 1. Evolution of a square 2D REV (a) initial state (b) after 20% of deformation (c) after 40% of deformation and (d) velocity norm after 40% of deformation

As results, in these cases, particles deform significantly over time, leading to increasing necks between particles and relative density. The influence of numerical parameters on mass conservation is studied in this work. These parameters are especially: compressibility coefficient, remeshing period, mixture law and the number of mesh nodes. Results show that the effect of compressibility coefficient is important. A compressibility coefficient  $C_k$  equal to zero for the powder particles would be ideal to minimize the loss of volume. However, this value would be synonymous of a too stiff mixture law. So  $10^{-10} \text{ Pa}^{-1}$  and  $10^{-2} \text{ Pa}^{-1}$  compressibility coefficient values are applied, respectively, to the powder particles and IPS domain. Moreover, when the remeshing period is extended, the conservation is better. Therefore, it is advisable that we perform remeshing only if interfaces of particles are in the situation to leave the refined part of the mesh. This reduces the computational cost and also limits the numerical diffusion due to the transport of variables during remeshing.

Using this initial formalism, several numerical difficulties appeared:

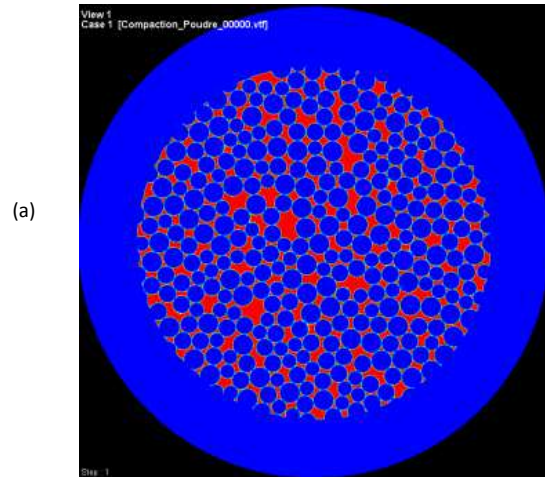
- unrefinement of the mesh at necks. In fact, considering a global distance function leads to the loss of the description of necks between particles because it just describes the envelope of the union of the particles and the mesh adaptation is performed at the isovalue zero of this function. The method used here, to solve this problem, is to use the classical technique of graph coloring. The idea is to color the particles of a graph (assigning each particle to a level-set function family) such that adjacent particles never share the same color (level-set function) with a minimal number of colors. This method allows keeping the description of the necks between particles and enabled us to limit the number of necessary level-set functions used to describe the particles.
- The consideration of a power law creep behavior for modeling the behavior of particles makes the resolution of the mechanical problem more difficult.
- Boundary condition problems in the top-left corner of the REV due to the introduction of two SD to apply BC.
- The control of the material conservation is one of the important points. The influence of various parameters on this observable has been studied. A Material loss around 2% was noted.

As a second approach, to avoid the problem of BC, a circular 2D REV is considered. An isostatic pressure is imposed on the external border of the SD. The numerical and physical parameters used for these simulations are presented in table 1. Given this configuration, the mean effective pressure particles is probably significantly different from the pressure applied on the boundary of the REV. For example, in the case of figure 2, a 3.5 ratio between the pressure applied and sustained by the particles is measured. The objective of this second approach is to study the deformation of particles in an isothermal case and also within the case of a cycle modulated from 800 to 1150 °C in one hour (close to the last hour of a rise in

pressure and temperature in a HIP cycle). To avoid borders effects, the computing of the average relative density of the REV is performed by calculating the volume (surface in 2D) of powder particles contained in a square situated far from the boundaries of the REV. Some important points from this numerical modelling of the HIP process at the mesoscopic scale can be highlighted: a good profile of relative density evolution (Fig. 3), a remarkable evolution of powder particles, especially in the center of the REV (Fig. 4) and an optimized material loss of around 2%. Fig. 4 illustrates the particles configuration after 1 hour cycle. A good densification is observed. It should be noted that velocity norm field is not homogeneous but depends essentially on the particles arrangement.

**Table 1. Numerical and physical parameters used**

K	SD	1075 MPa
	Particles	From 371 MPa to 580 MPa
	IPS	$10^{-3}$ MPa
m	SD	0.2
	Particles	From 0.198 to 0.495
	IPS	1
C <sub>K</sub>	SD	$10^{-10}$ (Pa <sup>-1</sup> )
	Particles	$10^{-10}$ (Pa <sup>-1</sup> )
	IPS	$10^{-2}$ (Pa <sup>-1</sup> )
Time step		1.5 s
h <sub>min</sub> (mesh size)		0,0012
remeshing period		30s
Pressure		From 80 MPa to 120 MPa
Number of elements		302159
Number of processors		32





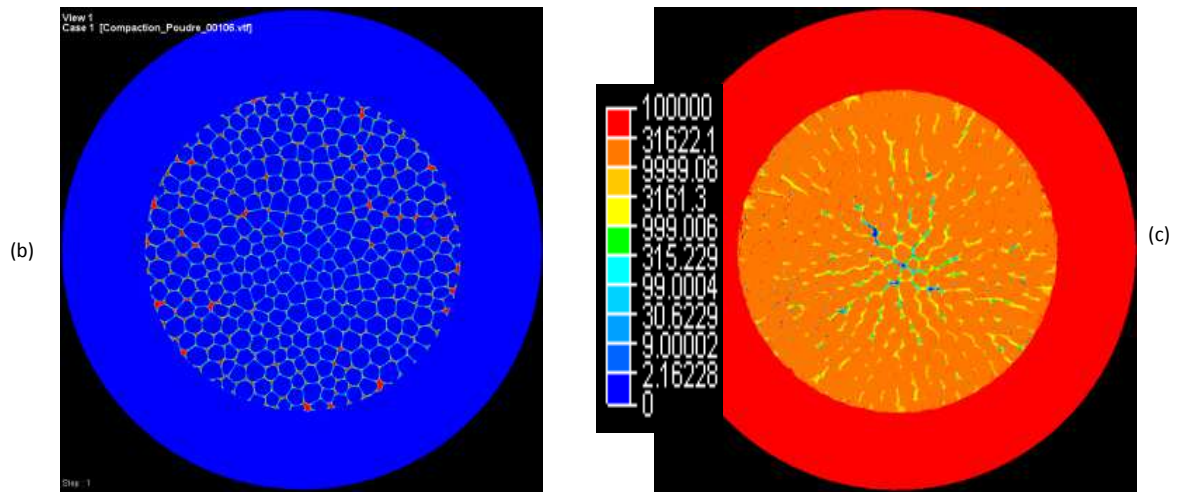


FIG 2. Evolution of a circular 2D REV: (a) initial state (b) after 22% of deformation and (c) pressure field after 22% of densification

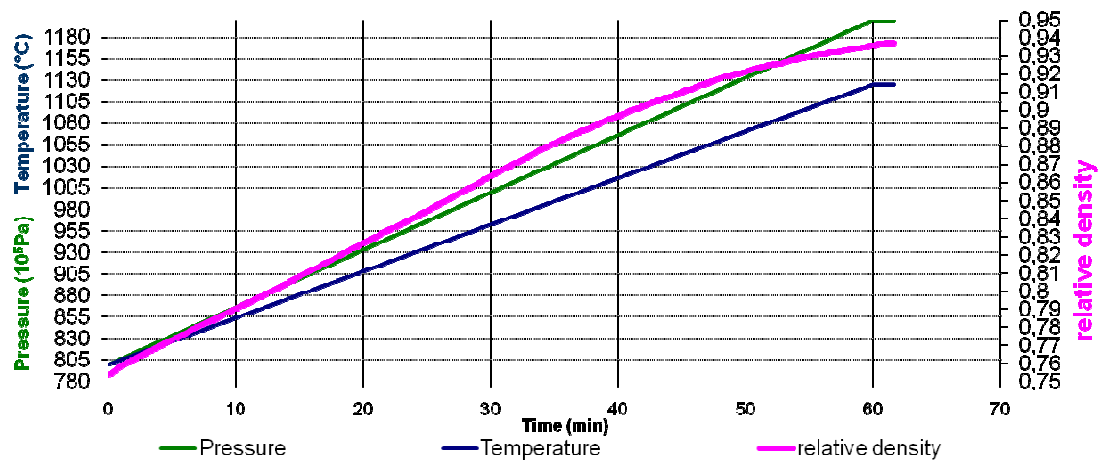


FIG 3. Relative density evolution for a cycle started from 800 °C to 1150°C in one hour

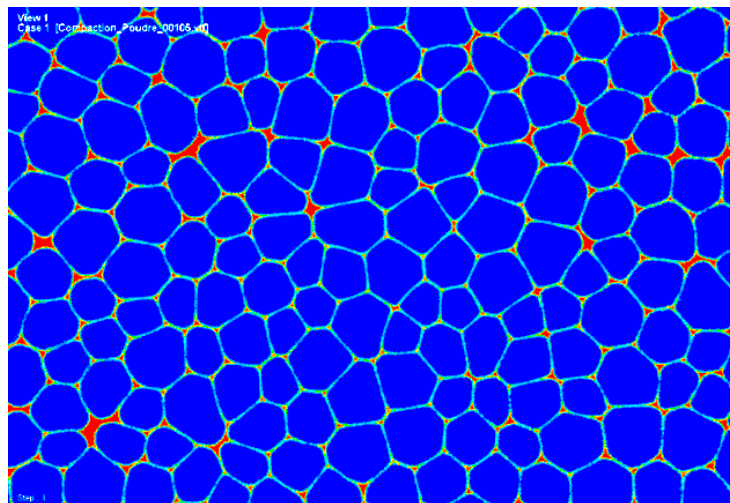


FIG 4. Zoom at the middle part for the circle REV after 1 hour HIPping

## **5. Conclusion**

This paper describes a robust finite element strategy based on a level set framework, coupled with an adaptive automatic remeshing technique, to model the power law creep mechanism of the HIP process. The densification behavior of stainless steel 316L powder during the last hour of a HIP cycle is considered. Firstly, a strategy to model the compaction of powder particles in 2D is presented. The evolution of relative density is investigated. The modelling of the different subdomains of REV (particles and IPS) was based on the power law creep and the resolution of Navier-Stokes compressible equations. The numerical model used is based on a fixed domain in which the interfaces between different subdomains are known only implicitly through the values of few distances functions defined on the entire domain. The physical properties of the different media were introduced through a mixture law. The proposed technique is directly usable in a 3D context. The present paper demonstrates the capability of the present work to simulate HIPing of particles powder in the REV scale. Current work addresses the modeling of a REV with a real granulometry and the improvement of the proposed technique to optimize numerical results and process parameters.

## **6. Acknowledgement**

This work was supported by AREVA group. It was carried out as a part of « Nuclear Materials » Chair proposed by AREVA and MINES ParisTech. This support is gratefully acknowledged.



## 7. References

- [Atkinson and Davis, 00] H.V. Atkinson and S. Davis, Fundamental aspects of hot isostatic pressing: an overview, *Metallurgical and Materials Transactions A*, 2000, vol. 31A, pp. 2981–3000.
- [Ransing and al., 00] R.S. Ransing, D.T. Gethin, A.R. Khoei, P. Mosbah, R.W. Lewis, Powder compaction modeling via the discrete and finite element method, *Materials and design*, 2000, vol. 21, pp. 263-269.
- [Choi and Gethin, 09] J.L. Choi et D.T. Gethin, A discrete element modeling and measurements for powder compaction, *Modelling and Simulation in Materials Science and Engineering*, 2009, vol. 17, pp. 1-22.
- [Helle and al., 85] A.S. Helle, K.E. Easterling et M.F. Ashby, Hot-isostatic pressing diagrams: New developments, *Acta Metallurgica*, 1985, vol. 33, pp. 2163-2174.
- [Wilkinson and Ashby, 75] D.S. Wilkinson, M.F. Ashby, Pressure sintering by power law creep, *Acta Metallurgica*, 1975, vol. 23, pp. 1277-1285.
- [Arzt and al., 83] E. Arzt, M.F. Ashby, and K.E. Easterling, Practical applications of hot-isostatic pressing diagrams: Four case studies, *Metallurgical Transactions A*, 1983, vol. 14A, pp. 211–221.
- [Bouaziz and al., 97] O. Bouaziz, C. Dellis, P. Stutz, Creation of a material data file for modelling of an austenitic stainless steel, *Proceedings of the International Workshop on Modelling of Metal Powder Forming Processes*, Grenoble, pp. 67–75.
- [Kim and Jeon, 98] K.T. Kim and Y.C. Jeon, Densification behavior of 316L stainless steel powder under high temperature, *Materials Science and Engineering*, 1997, vol. 245 A, pp. 64-71, 1998.
- [Coupez, 06] T. Coupez, Réinitialisation convective et locale des fonction Level Set pour le mouvement de surfaces et d'interfaces, *Journées activités universitaire de mécanique*, La Rochelle, 2006, pp.1-9.
- [Bernacki and al., 09] M. Bernacki, H. Resk, T. Coupez and R. Logé, Finite element model of primary recrystallization in polycrystalline aggregates using a level set framework, *Modelling and Simulation in Materials Science and Engineering*, 2009, vol 17, pp.1-22.
- [Hitti and al., 12] K. Hitti, P. Laure, T. Coupez, L. Silva, M. Bernacki, Fast generation of complex statistical Representative Elementary Volumes (REV's) in a finite element context, submitted to *Journal of Computational Physics*.